

# Switching-Reference Voltage Control for Distribution Systems with AI-Training Data Centers

Mingyuan Yan, Trager Joswig-Jones, Baosen Zhang, Yize Chen, Wenqi Cui

**Abstract**—Large-scale AI training workloads in modern data centers exhibit rapid and periodic power fluctuations, which may induce significant voltage deviations in power distribution systems. Existing voltage regulation methods, such as droop control, are primarily designed for slowly varying loads and may therefore be ineffective in mitigating these fast fluctuations. In addition, repeated control actions can incur substantial cost. To address this challenge, this paper proposes a decentralized switching-reference voltage control framework that exploits the structured behavior of AI training workloads. We establish conditions for voltage convergence and characterize an effective reference design that aligns with the dominant operating level of the AI training workload. The switching rule for voltage references is implemented solely based on local voltage measurements, enabling simple local implementation while significantly reducing control effort. Simulation studies demonstrate that the proposed method substantially reduces both voltage deviations and reactive control effort, while remaining compatible with internal data center control strategies without requiring extensive coordination.

## I. INTRODUCTION

The rapid growth of artificial intelligence (AI) has led to the deployment of increasingly large training workloads in hyperscale data centers. Empirical scaling laws show that model performance improves predictably with increasing model size, data, and computational budget [1], [2]. As a consequence, the electric power demand driving AI training has also grown rapidly [3]. At the same time, the scale and geographic concentration of modern data centers make their power consumption an increasingly important factor in power system operation.

At the distribution level, large data centers introduce a new class of highly dynamic loads. For example, recent industrial studies report that synchronized AI training workloads can produce large, periodic active-power ramps [4]. Unlike conventional electricity demand, which typically evolves gradually over time, AI training workloads can produce large and rapid power swings in the aggregate demand of a data center. When such loads are connected to a distribution feeder, these power swings propagate through the network and cause large voltage deviations. Without effective regulation, voltages may exceed their allowable limits.

M. Yan and W. Cui are with the Department of Electrical and Computer Engineering, New York University {my3188, wenqicui}@nyu.edu

T. Jones and B. Zhang are with the Department of Electrical and Computer Engineering, University of Washington Seattle {joswitra, zhangbao}@uw.edu

Y. Chen is with the Department of Electrical and Computer Engineering, University of Alberta {yize.chen}@ualberta.ca

The authors are partially supported by the Henry Luce Foundation.

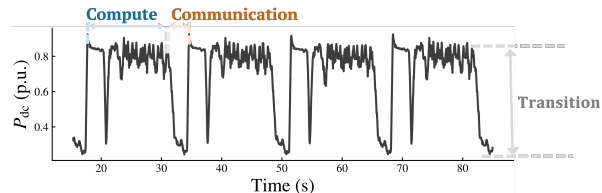


Fig. 1. Per unit power readings from an at-scale training job on DGX H100 racks [4].

One common approach to voltage regulation in distribution systems is the control of reactive power throughout the network. Traditionally, this has been achieved using mechanical control devices such as tap-changing transformers, which are not suitable for frequent adjustments due to equipment lifespan limitations. Inverter-based resources, such as energy storage systems, can update their reactive power setpoints much more rapidly and have therefore emerged as valuable resources for voltage regulation. Accordingly, voltage droop control and its variants have been widely proposed to exploit this capability [5]–[8]. However, these methods are primarily designed for slowly varying loads and are therefore not well suited to AI training workloads with rapid power fluctuations. Beyond grid-side voltage regulation, recent studies have also treated data centers as active participants by leveraging internal infrastructure for voltage support, including workload-aware power capping [9], distributed server-level power modulation [10], [11], coordinated control of UPS and cooling systems [12], and GPU utilization control via batch size modulation [13]. Some works have further considered coordination with external grid assets by introducing new interface infrastructure, such as grid-forming battery energy storage systems providing line-interactive UPS functionality and dynamic active power support [14], [15], as well as coordination with external flexible resources like EV charging stations [16]. However, these approaches overlook the underlying power dynamics of modern AI training workloads, leading to unnecessarily large control effort while providing limited improvement in worst-case voltage deviations.

A representative AI training power trace is shown in Fig. 1, characterized by rapid ramps and periodic fluctuations. This distinctive pattern arises from the distributed training of large AI models across multiple GPU racks: power demand increases substantially during computation in each training iteration and then drops sharply during communication. These abrupt load transitions constitute the dominant source of voltage deviations along the feeder. Since the most severe voltage violations arise during these abrupt transitions, existing regulation methods designed for smoothly varying loads may not respond sufficiently fast or deliver effective

control actions to mitigate the worst violations. In addition, responding to repeated large power fluctuations may incur substantial control costs. In this work, we aim to answer the following question: *How should we design a voltage control law to mitigate voltage deviations induced by AI training workloads, while avoiding excessive control effort?*

In this paper, we propose a novel decentralized voltage control framework with a switching reference that responds to the periodic behavior of AI training workloads. The key idea is to exploit the structured switching dynamics of such loads to reduce voltage deviations with minimal control effort. We first characterize the two-mode structure of large-scale AI training workloads, and then design a switching-reference droop controller that aligns the voltage reference with the dominant operating level of the data center load. On this basis, we establish conditions for voltage convergence and characterize when the placement of voltage references can effectively reduce voltage deviations. We further develop a rule for switching voltage references based solely on local voltage measurements, enabling simple local implementation while significantly reducing control effort. Case studies demonstrate that the proposed approach substantially reduces voltage deviations and reactive control effort compared with conventional fixed-reference droop control, and remains effective in scenarios with multiple data centers and when coordinated with data-center-side load smoothing.

## II. NETWORK MODEL AND PROBLEM FORMULATION

### A. Network Model and Data Center Power Characteristics

We consider a radial distribution network with  $n$  buses, where a large data center is connected at the  $j$ -th bus. Let  $\mathbf{v}_t, \mathbf{p}_t, \mathbf{q}_t \in \mathbb{R}^n$  denote the vectors of bus voltage magnitudes, active power injections, and reactive-power injections at time  $t$ . Following common practice, voltages are normalized so that the nominal value at all buses is 1 per unit (p.u.).

We adopt the LinDistFlow model in [6], [17] to characterize the bus voltages

$$\mathbf{v}_t = \mathbf{R}\mathbf{p}_t + \mathbf{X}\mathbf{q}_t + \mathbf{1}, \quad (1)$$

where  $\mathbf{1}$  is the all-ones vector and  $\mathbf{R}, \mathbf{X} \in \mathbb{R}^{n \times n}$  are positive definite matrices determined by the network topology and line impedances.

Modern synchronized training workloads exhibit temporal structure in active power consumption that differs fundamentally from conventional slowly varying demand. As shown in Fig. 1, the aggregate data center power exhibits repeated switching between two dominant operating levels with abrupt transitions. We refer to the high-power phase (forward and backward propagation) as the *compute phase*, and to the lower-power phase (synchronization and checkpointing) as the *communication phase*. Because accelerators (i.e., GPUs or TPUs) operate synchronously, the aggregate demand transitions collectively between these two phases.

Motivated by this temporal structure, we model active power injection at the data center bus  $j$  as

$$p_{j,t} = \bar{p}_j(m_t) + w_t, \quad |w_t| \leq \bar{w}(m_t), \quad (2)$$

where  $m_t \in \{0, 1\}$  denote the mode, with 0 for communication and 1 for computation. The injections  $\bar{p}_j(0)$  and  $\bar{p}_j(1)$  are the corresponding average demand, while  $w_t$  captures intra-phase fluctuations, and  $\bar{w}(m_t)$  specifies a mode-dependent bound on these fluctuations.

During large-scale AI training, short-term active power variation is dominated by training workload within the data center, and we regard the power injections at other buses as remaining nearly constant. Let  $\bar{\mathbf{p}}(0), \bar{\mathbf{p}}(1) \in \mathbb{R}^n$  denote the network average active power injections associated with the communication and computation modes, respectively. For a data center connected at bus  $j$ , the two network injection profiles differ only at that bus, i.e.,  $\bar{\mathbf{p}}(0) - \bar{\mathbf{p}}(1) = (\bar{p}_j(0) - \bar{p}_j(1))\mathbf{e}_j$  with  $\mathbf{e}_j$  being the  $j$ -th standard basis vector.

### B. Voltage Control and Challenges

Large and rapid variations in data center power usage affect voltages throughout the system and may drive them toward or beyond acceptable operating limits (e.g., within  $\pm 5\%$  of nominal) [18].

Reactive power control is commonly used to regulate the voltage in distribution systems. A widely adopted approach is decentralized Volt-VAR droop control [5], [7], [19], in which inverter-based resources adjust reactive power injections based on local voltage measurements. In discrete time, a typical droop update can be written as

$$\mathbf{q}_{t+1} = \mathbf{q}_t - \mathbf{K}(\mathbf{v}_t - \mathbf{1}), \quad (3)$$

where  $\mathbf{K} = \text{diag}(k_1, \dots, k_n)$  with  $k_i > 0$ .

This type of droop control only uses current information to drive voltages towards a fixed reference (e.g., 1 p.u. in (3)). However, when applied to step power transitions induced by AI training workloads, the controller repeatedly reacts to each transition without accounting for the underlying two-mode structure of the training workload. As a result, large voltage deviations can persist during frequent mode transitions.

To address the above challenges, we propose a decentralized grid-side voltage control framework that exploits the structured power dynamics of AI training workloads. The key idea is to incorporate the characteristic step power changes of data centers into the design of voltage control, as illustrated in Fig. 1. As we will show, by aligning voltage regulation with this structured load behavior, voltages can be maintained within the desired range with much smaller and less frequent reactive power injections. Importantly, the proposed controller operates independently of data-center-side optimization. If internal resources such as battery storage partially smooth the active power load [20], the grid-side controller remains effective, and is compatible with internal data center control strategies.

## III. GRID-SIDE VOLTAGE CONTROL

### A. Control Law with Time-varying Voltage References

Our proposed controller retains the form

$$\mathbf{q}_{t+1} = \mathbf{q}_t - \mathbf{K}(\mathbf{v}_t - \mathbf{v}_t^{\text{ref}}), \quad (4)$$

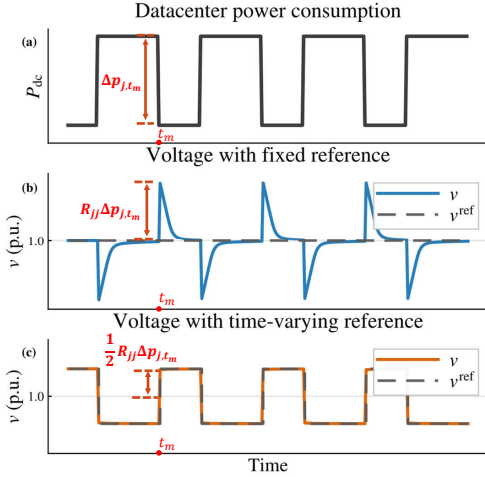


Fig. 2. Voltage response to step-like data center power transitions. (a) Active power profile at the data center bus, where the power switches between two operating levels and exhibits a step change of  $\Delta p_{j,t_m}$  at each transition. (b) Voltage trajectory under decentralized droop control with a fixed reference  $v^{\text{ref}} \equiv 1$ . Each transition induces a voltage shift approximately  $R_{jj}\Delta p_{j,t_m}$ . (c) Voltage trajectory with a time-varying reference aligned with the data center mode switching. By shifting the reference, the worst post-transition voltage deviation is reduced to approximately  $\frac{1}{2}R_{jj}\Delta p_{j,t_m}$ .

with the key difference from (3) being that the reference used to compute the feedback error term,  $v_i^{\text{ref}}$ , is now time-varying. To see why this reference should be set dynamically rather than be held constant, we note that the voltage change between two neighboring time steps satisfies

$$\mathbf{v}_{t+1} = \mathbf{v}_t + \mathbf{R} \Delta \mathbf{p}_t + \mathbf{X} \Delta \mathbf{q}_t, \quad (5)$$

where  $\Delta \mathbf{p}_t := \mathbf{p}_{t+1} - \mathbf{p}_t$  and  $\Delta \mathbf{q}_t := \mathbf{q}_{t+1} - \mathbf{q}_t$ .

We start by illustrating why conventional droop control with a fixed reference of 1 p.u. may cause large voltage deviations. Consider the data center load abstracted in Fig. 2(a), where intra-mode fluctuations are smoothed out. Let  $t_m$  denote a time at which the data center switches between the two modes and the power increment is  $\Delta p_{j,t_m} = p_{j,t_m+1} - p_{j,t_m}$ . Because  $\Delta p_{j,t_m}$  is large, it induces a significant voltage deviation. However, conventional droop methods only respond after a voltage change has occurred, and therefore cannot prevent these types of large voltage swings as shown in Fig. 2(b). This issue cannot be solved simply by increasing the droop gain: a larger gain accelerates the decay but does not reduce the initial transient spike.

Motivated by this observation, we propose to assign different voltage reference levels for the two data center operating modes so that the reference effectively shifts between two levels to preempt the large load changes. As shown in Fig. 2(c), this time-varying reference effectively shifts between two levels, allowing part of the voltage change induced by the power transition to be absorbed by the reference itself. For example, right after a transition, the peak voltage deviation is approximately  $|R_{jj}\Delta p_{j,t_m}|$ . However, choosing a reference to  $v_{j,t_m}^{\text{ref}} = 1 - \frac{1}{2}R_{jj}\Delta p_{j,t_m}$  yields a post-transition voltage  $v_{j,t_m+1} \approx 1 + \frac{1}{2}R_{jj}\Delta p_{j,t_m}$ , reducing the peak deviation to roughly half that under the fixed reference.

In particular, we implement this time-varying reference

as a switching reference that alternates between two levels. More formally, we parameterize the reference as

$$v_{i,t}^{\text{ref}} = 1 + s_{i,t} v_i^{\text{amp}}, \quad (6)$$

where  $s_{i,t}^t \in \{-1, +1\}$  selects one of the two reference levels, and  $v_i^{\text{amp}} \in \mathbb{R}_{\geq 0}$  determines their magnitude. We will later show how to set  $s_{i,t}^t$  such that the reference of each bus  $i$  switches between  $\pm v_i^{\text{amp}}$  depending on the data center mode  $m_t$ .

In practice, voltage fluctuations exist within each operating mode and may have different magnitudes (e.g., voltage variations during the compute phase are larger than those during the communication phase). To accommodate this asymmetry, we introduce a bias term that allows the midpoint of the two reference levels to shift. Accordingly, we generalize (6) to

$$v_{i,t}^{\text{ref}} = v_i^{\text{bias}} + s_{i,t} v_i^{\text{amp}}, \quad (7)$$

where  $v_i^{\text{bias}} \in \mathbb{R}$  is the bias of voltage reference at bus  $i$ .

Under this parameterization, the two reference levels for each bus  $i$  are centered at  $v_i^{\text{bias}}$  and separated by  $2v_i^{\text{amp}}$ . The remaining question is how these reference levels should be chosen so that the steady-state voltage shift induced by active power variation is incorporated into the reference itself.

### B. Switching Law and Closed-Loop Voltage Deviation Analysis

We now analyze the closed-loop voltage deviation, and show how the references should be chosen to reduce the worst-case voltage deviation from its nominal value.

Substituting (4) into the LinDistFlow model in (1), the voltage deviation relative to the reference evolves as

$$\mathbf{v}_{t+1} - \mathbf{v}_{t+1}^{\text{ref}} = (\mathbf{I} - \mathbf{X}\mathbf{K})(\mathbf{v}_t - \mathbf{v}_t^{\text{ref}}) + \mathbf{d}_t, \quad (8)$$

where  $\mathbf{d}_t := \mathbf{R}\Delta \mathbf{p}_t - \Delta \mathbf{v}_t^{\text{ref}}$ ,  $\Delta \mathbf{p}_t := \mathbf{p}_{t+1} - \mathbf{p}_t$ , and  $\Delta \mathbf{v}_t^{\text{ref}} := \mathbf{v}_{t+1}^{\text{ref}} - \mathbf{v}_t^{\text{ref}}$ . The detailed derivation is provided in Appendix A.

The error between  $\mathbf{v}_{t+1} - \mathbf{v}_{t+1}^{\text{ref}}$  depends on both terms on the right-hand side in (8). Therefore, we design  $\mathbf{K}$  to ensure closed-loop contraction and bound the size of the disturbance  $\mathbf{d}_t$ . We have the following theorem<sup>1</sup>:

**Theorem 1** (Convergence of voltage deviation). *If the diagonal gain matrix  $\mathbf{K}$  satisfies  $0 \prec \mathbf{K} \prec 2\mathbf{X}^{-1}$ , then there exist a nonnegative matrix  $\mathbf{C}$  and a constant  $0 < \epsilon < 1$  such that for any initial time  $t_0$  and all  $t \geq t_0$ ,*

$$|\mathbf{v}_t - \mathbf{v}_t^{\text{ref}}| \leq \mathbf{C} \epsilon^{t-t_0} |\mathbf{v}_{t_0} - \mathbf{v}_{t_0}^{\text{ref}}| + \sum_{\tau=t_0}^{t-1} \mathbf{C} \epsilon^{t-1-\tau} |\mathbf{d}_\tau|. \quad (9)$$

*In particular, for any  $\bar{\mathbf{d}}$  where  $|\mathbf{d}_t| \leq \bar{\mathbf{d}}$  for all  $t$ ,*

$$\limsup_{t \rightarrow \infty} |\mathbf{v}_t - \mathbf{v}_t^{\text{ref}}| \leq \frac{1}{1-\epsilon} \mathbf{C} \bar{\mathbf{d}}. \quad (10)$$

*Proof.* Let  $\mathbf{e}_t := \mathbf{v}_t - \mathbf{v}_t^{\text{ref}}$  and  $\mathbf{A} := \mathbf{I} - \mathbf{X}\mathbf{K}$ . Then (8) becomes  $\mathbf{e}_{t+1} = \mathbf{A}\mathbf{e}_t + \mathbf{d}_t$ . By Lemma 4 in Appendix B, there

<sup>1</sup>Here  $|\cdot|$  denotes elementwise absolute value. Vector and matrix inequalities are interpreted elementwise, and  $\limsup$  applied to vectors is also understood elementwise.

exist a nonnegative matrix  $\mathbf{C} \geq \mathbf{0}$  and a constant  $0 < \epsilon < 1$  such that  $|\mathbf{A}^k| \leq \mathbf{C} \epsilon^k$  for all  $k \geq 0$ . Unrolling the recursion from  $t_0$  gives  $\mathbf{e}_t = \mathbf{A}^{t-t_0} \mathbf{e}_{t_0} + \sum_{\tau=t_0}^{t-1} \mathbf{A}^{t-1-\tau} \mathbf{d}_\tau$ . Taking elementwise absolute values yields  $|e_t| \leq |\mathbf{A}^{t-t_0}| |e_{t_0}| + \sum_{\tau=t_0}^{t-1} |\mathbf{A}^{t-1-\tau}| |\mathbf{d}_\tau|$ . Using  $|\mathbf{A}^k| \leq \mathbf{C} \epsilon^k$  gives  $|e_t| \leq \mathbf{C} \epsilon^{t-t_0} |e_{t_0}| + \sum_{\tau=t_0}^{t-1} \mathbf{C} \epsilon^{t-1-\tau} |\mathbf{d}_\tau|$ .

If  $|\mathbf{d}_t| \leq \bar{\mathbf{d}}$  for all  $t$ , then  $|e_t| \leq \mathbf{C} \epsilon^{t-t_0} |e_{t_0}| + \mathbf{C} \sum_{\ell=0}^{t-1-t_0} \epsilon^\ell \bar{\mathbf{d}}$ . Since  $0 < \epsilon < 1$ , letting  $t \rightarrow \infty$  gives  $\epsilon^{t-t_0} |e_{t_0}| \rightarrow 0$ ,  $\sum_{\ell=0}^{t-1-t_0} \epsilon^\ell \rightarrow \frac{1}{1-\epsilon}$ . Substituting  $\mathbf{e}_t = \mathbf{v}_t - \mathbf{v}_t^{\text{ref}}$  yields (10).  $\square$

Theorem 1 shows that the voltage deviation  $|\mathbf{v}_t - \mathbf{v}_t^{\text{ref}}|$  is driven by the disturbance  $\mathbf{d}_t = \mathbf{R} \Delta \mathbf{p}_t - \Delta \mathbf{v}_t^{\text{ref}}$ . For conventional voltage control with fixed references,  $\mathbf{d}_t = \mathbf{R} \Delta \mathbf{p}_t$  and therefore the large fluctuation of load (i.e., large  $\Delta \mathbf{p}_t$ ) results in large voltage deviations.

Next, we show how designing switching references can reduce the magnitude of  $\mathbf{d}_t$ , thereby limiting the steady-state voltage deviation. The active-power increment at the data center can be decomposed as  $\Delta p_{j,t} = (\bar{p}_j(m_{t+1}) - \bar{p}_j(m_t)) + (w_{t+1} - w_t)$ , where the first term represents the structured shift of power caused by mode transitions of data center loads, and the second term captures the intra-mode fluctuations. To cancel the voltage deviation induced from mode transitions, we design the reference to depend only on the data center mode  $m_t$  rather than directly on time  $t$ ,

$$\mathbf{v}_t^{\text{ref}} = \bar{\mathbf{v}}^{\text{ref}}(m_t), \quad (11)$$

where  $\bar{\mathbf{v}}^{\text{ref}}(0)$  and  $\bar{\mathbf{v}}^{\text{ref}}(1)$  denote the reference voltages associated with the two data center modes. From (1), the voltage change induced by a data center power step is  $\Delta \mathbf{v}_{\text{mode}} := \mathbf{R}(\bar{\mathbf{p}}(0) - \bar{\mathbf{p}}(1))$ . The next proposition characterizes conditions on the choice of voltage references under which the disturbance induced by mode switching can be canceled.

**Proposition 2** (Voltage reference switching). *Let the reference design follow (11) and  $\Delta \mathbf{v}_{\text{mode}} := \mathbf{R}(\bar{\mathbf{p}}(0) - \bar{\mathbf{p}}(1))$ . If the references for two modes satisfy*

$$\bar{\mathbf{v}}^{\text{ref}}(0) = \mathbf{b} + \frac{1}{2} \Delta \mathbf{v}_{\text{mode}}, \quad \bar{\mathbf{v}}^{\text{ref}}(1) = \mathbf{b} - \frac{1}{2} \Delta \mathbf{v}_{\text{mode}}, \quad (12)$$

then the disturbance term  $\mathbf{d}_t$  in (8) reduces to  $\mathbf{d}_t = \mathbf{r}_j(w_{t+1} - w_t)$ , where  $\mathbf{r}_j$  denotes the  $j$ th column of  $\mathbf{R}$ .

*Proof.* Since  $\Delta \mathbf{p}_t = \mathbf{e}_j \Delta p_{j,t}$ , multiplying by  $\mathbf{R}$  gives

$$\mathbf{R} \Delta \mathbf{p}_t = \mathbf{r}_j(\bar{p}_j(m_{t+1}) - \bar{p}_j(m_t) + w_{t+1} - w_t).$$

Under the reference design (11),  $\Delta \mathbf{v}_t^{\text{ref}} = \bar{\mathbf{v}}^{\text{ref}}(m_{t+1}) - \bar{\mathbf{v}}^{\text{ref}}(m_t)$ . By (12), the difference between the two reference levels matches the voltage change induced by the mode transition, and thus  $\bar{\mathbf{v}}^{\text{ref}}(m_{t+1}) - \bar{\mathbf{v}}^{\text{ref}}(m_t) = \mathbf{r}_j(\bar{p}_j(m_{t+1}) - \bar{p}_j(m_t))$ . Substituting into  $\mathbf{d}_t = \mathbf{R} \Delta \mathbf{p}_t - \Delta \mathbf{v}_t^{\text{ref}}$  yields  $\mathbf{d}_t = \mathbf{r}_j(w_{t+1} - w_t)$ .  $\square$

Proposition 2 shows that a proper choice of the references can reduce the disturbance magnitude  $|\mathbf{d}_t|$ , and consequently the voltage deviation  $|\mathbf{v}_t - \mathbf{v}_t^{\text{ref}}|$ . Note that the goal of voltage control is to reduce voltage deviation from its nominal

voltage at 1 p.u. We further characterize how shifting the bias for voltage references can further reduce the worst-case steady-state voltage deviation from the nominal voltage.

In particular, under the reference design (11)–(12), the steady-state extrema  $\mathbf{v}^+(\mathbf{b})$  and  $\mathbf{v}^-(\mathbf{b})$  induced by the current bias  $\mathbf{b}$  provide the information needed to correct the bias and reduce the worst-case steady-state deviation. This observation is formalized in the following proposition.

**Proposition 3** (Bias shifting). *Under the reference design (11)–(12), define for each mode  $m \in \{0, 1\}$  the steady-state voltage extrema  $\mathbf{v}^+(m, \mathbf{b}) := \limsup_{t \rightarrow \infty} \mathbf{v}_t$  and  $\mathbf{v}^-(m, \mathbf{b}) := \liminf_{t \rightarrow \infty} \mathbf{v}_t$  along trajectories with fixed mode  $m_t \equiv m$ . The corresponding steady-state extrema across two modes are  $\mathbf{v}^+(\mathbf{b}) := \max\{\mathbf{v}^+(0, \mathbf{b}), \mathbf{v}^+(1, \mathbf{b})\}$  and  $\mathbf{v}^-(\mathbf{b}) := \min\{\mathbf{v}^-(0, \mathbf{b}), \mathbf{v}^-(1, \mathbf{b})\}$ . Then the bias that minimizes the worst-case steady-state voltage deviation from the nominal value is*

$$\mathbf{b}^* = \mathbf{b} - \left( \frac{\mathbf{v}^+(\mathbf{b}) + \mathbf{v}^-(\mathbf{b})}{2} - \mathbf{1} \right). \quad (13)$$

*Proof.* For each fixed mode  $m \in \{0, 1\}$ , let  $\mathbf{v}^+(m, \mathbf{b})$  and  $\mathbf{v}^-(m, \mathbf{b})$  denote the corresponding steady-state voltage extrema under the bias  $\mathbf{b}$ . By definition, the overall steady-state extrema are  $\mathbf{v}^+(\mathbf{b}) = \max\{\mathbf{v}^+(0, \mathbf{b}), \mathbf{v}^+(1, \mathbf{b})\}$  and  $\mathbf{v}^-(\mathbf{b}) = \min\{\mathbf{v}^-(0, \mathbf{b}), \mathbf{v}^-(1, \mathbf{b})\}$ . Hence  $\limsup_{t \rightarrow \infty} |\mathbf{v}_t - \mathbf{1}| = \max\{\mathbf{v}^+(\mathbf{b}) - \mathbf{1}, \mathbf{1} - \mathbf{v}^-(\mathbf{b})\}$ .

Now shift the bias from  $\mathbf{b}$  to  $\mathbf{b} + \delta \mathbf{b}$ . Under the reference parameterization  $\mathbf{v}^{\text{ref}}(0) = \mathbf{b} + \frac{1}{2} \Delta \mathbf{v}_{\text{mode}}$  and  $\mathbf{v}^{\text{ref}}(1) = \mathbf{b} - \frac{1}{2} \Delta \mathbf{v}_{\text{mode}}$ , this shift translates both reference levels by the same amount  $\delta \mathbf{b}$ . Therefore, for each fixed mode  $m$ , the corresponding steady-state voltage trajectory is translated by  $\delta \mathbf{b}$ , and thus  $\mathbf{v}^+(m, \mathbf{b} + \delta \mathbf{b}) = \mathbf{v}^+(m, \mathbf{b}) + \delta \mathbf{b}$  and  $\mathbf{v}^-(m, \mathbf{b} + \delta \mathbf{b}) = \mathbf{v}^-(m, \mathbf{b}) + \delta \mathbf{b}$ . Taking the componentwise maximum and minimum over  $m \in \{0, 1\}$  gives  $\mathbf{v}^+(\mathbf{b} + \delta \mathbf{b}) = \mathbf{v}^+(\mathbf{b}) + \delta \mathbf{b}$  and  $\mathbf{v}^-(\mathbf{b} + \delta \mathbf{b}) = \mathbf{v}^-(\mathbf{b}) + \delta \mathbf{b}$ .

The worst-case steady-state deviation under the shifted bias becomes  $\max\{\mathbf{v}^+(\mathbf{b}) + \delta \mathbf{b} - \mathbf{1}, \mathbf{1} - (\mathbf{v}^-(\mathbf{b}) + \delta \mathbf{b})\}$ . For the  $i$ -th entry, the first term increases with  $\delta b_i$  while the second decreases, so the minimum is attained when the two terms are equal. This gives  $\delta \mathbf{b} = \mathbf{1} - \frac{1}{2}(\mathbf{v}^+(\mathbf{b}) + \mathbf{v}^-(\mathbf{b}))$ , which directly yields the update of bias in (13).  $\square$

### C. Measurement-Based Reference Adaptation

In practice, neither the data center mode  $m_t$ , the abrupt voltage change  $\Delta \mathbf{v}_{\text{mode}}$  from the mode switching, nor the optimal bias  $\mathbf{b}^*$  is directly available to the grid controller. We therefore construct a measurement-based reference using only local voltage observations.

Fortunately, both the abrupt voltage change  $\Delta \mathbf{v}_{\text{mode}}$  induced by mode transitions and the voltage extrema for bias correction can be approximated from recent voltage measurements. We therefore maintain the most recent  $L$  voltage samples for each bus  $i$ ,  $\mathcal{W}_{i,t} := \{v_{i,t-\ell} \mid \ell = 0, \dots, L-1\}$ .

Specifically, for each bus  $i$ , we use the reference structure characterized in Proposition 2 and 3 to construct the time-varying reference

$$v_{i,t}^{\text{ref}} = v_{i,t}^{\text{bias}} + s_{i,t} v_{i,t}^{\text{amp}}, \quad (14)$$

where  $v_{i,t}^{\text{bias}}$ ,  $s_{i,t}$ , and  $v_{i,t}^{\text{amp}}$  serve as estimates of the bias  $b_i$ , mode  $m_t$  and  $\frac{1}{2}\Delta v_{\text{mode},i}$ , respectively.

1) *Amplitude Update*: Guided by Proposition 2, we set  $v_{i,t}^{\text{amp}}$  equal to  $\frac{1}{2}\Delta v_{\text{mode},i}$ , which is the step voltage change resulting from the mode transition. We therefore adapt this value online using the largest per-step voltage change in the past window. Let  $L_a \leq L$  denote the window length used for amplitude estimation. If  $L_a$  is sufficiently long to include a mode transition, the window  $\mathcal{W}_{i,t}$  contains at least one recent transition, and the largest one-step voltage change within this window  $\max_{0 \leq \ell \leq L_a-2} |v_{i,t-\ell} - v_{i,t-\ell-1}|$  provides an estimate of the voltage change  $\Delta v_{\text{mode},i}$ . The amplitude is therefore updated as

$$v_{i,t}^{\text{amp}} = \frac{1}{2} \max_{0 \leq \ell \leq L_a-2} |v_{i,t-\ell} - v_{i,t-\ell-1}|. \quad (15)$$

2) *Bias Update*: Proposition 3 shows that the optimal bias can be determined from the steady-state voltage extrema using (13). Since these extrema are not directly observable, we approximate them from recent voltage measurements over a horizon  $L_b \leq L$ . Let  $\mathcal{W}_{i,t}$  denote the corresponding measurement window. If  $L_b$  is sufficiently long relative to the typical interval between mode transitions, the window  $\mathcal{W}_{i,t}$  captures the voltage range produced by the two operating modes. The midpoint of this range therefore provides an estimate of the bias update  $\Delta b$  in Proposition 3

$$\Delta b_{i,t} = \frac{1}{2} \left( \max_{0 \leq \ell \leq L_b-1} v_{i,t-\ell} + \min_{0 \leq \ell \leq L_b-1} v_{i,t-\ell} \right) - 1.$$

The bias is then updated incrementally as

$$v_{i,t+1}^{\text{bias}} = v_{i,t}^{\text{bias}} - \eta_b \Delta b_{i,t}, \quad (16)$$

where  $\eta_b \in (0, 1]$  is a smoothing gain. Note that  $\eta_b = 1$  in (13). Here we instead use a smaller gain to reduce the influence of outdated extrema that may remain in the finite window until replaced by newer samples. A smaller  $\eta_b$  reduces the effect of such stale extrema, while a larger  $\eta_b$  tracks recent changes more aggressively.

3) *Sign Selection*: The sign  $s_{i,t} \in \{-1, +1\}$  acts as a local estimate of the unknown data center mode  $m_t$ , enabling a decentralized approximation of (11) using only local voltage measurements. We choose:

$$s_{i,t} = \begin{cases} +1, & v_{i,t} > v_{i,t}^{\text{bias}}, \\ -1, & \text{otherwise.} \end{cases} \quad (17)$$

Because the bias approximates the midpoint between the two operating levels and intra-phase fluctuations are typically much smaller than the level separation, the voltage remains consistently above or below the bias within each phase, providing a simple decentralized rule for reference selection.

The above construction does not depend on a particular workload, model scale, or switching period. Different AI training jobs or internal data center controls may lead to different phase durations and transition magnitudes. Since these changing power patterns are reflected in the most recent voltage measurements, the measurement-based implementation enables the controller to adapt effectively to variations in the power profile. As will be demonstrated in the case study,

the proposed controller can accommodate disturbances from multiple data centers, as well as changes in the data center load profile induced by internal power-smoothing control.

## IV. EXPERIMENTS

### A. Simulation Setup

We evaluate the proposed method on the IEEE 33-bus distribution feeder [17]. The system is simulated with time step  $\Delta t_{\text{sim}} = 0.1\text{s}$ , at which voltage states and active power injections are updated. Reactive power control operates on a slower time scale, with updates applied every  $\Delta t_{\text{ctrl}} = 1.0\text{s}$  while holding reactive injections constant between control instants. This multi-time-scale implementation reflects practical inverter-based regulation, where measurement, filtering, and actuation occur at a slower rate than the underlying electrical dynamics [21].

For the proposed switching reference method, both the bias-update window and the amplitude-estimation window are set to 120s, i.e.,  $L_a = L_b = 120\text{s}$ . We compare the proposed method with the linear incremental voltage control in (3), which employs a fixed voltage reference of 1 p.u. For both methods, we adopt a symmetric deadband of 0.02 p.u. and per-update reactive power saturation of 0.01 p.u., consistent with the Volt-VAR standard specified in IEEE 1547 [5]. Moreover, the linear droop gain  $\mathbf{K}$  is set identical in both methods.

Simulations use an approximately 45-minute power trace corresponding to the aggregate GPU power consumption of a data center workload, collected during synchronous distributed training of the LLaMA-2-70B model [22] with a QLoRA configuration [23] on a 4×H200 GPU server. The synchronized training workflow induces repeatable compute/communication phase alignment and periodic patterns in the aggregate power trace. Hardware accelerators mainly scale the magnitude of the load but do not significantly change its temporal structure.

### B. Decentralized Grid-Side Control

Fig. 3 compares the conventional fixed-reference droop control with the proposed switching-reference control when a data center is connected to bus 22. Under fixed-reference control, control actions repeatedly reach the per-update limit, indicating sustained saturation of the control action. The resulting voltage trajectory exhibits persistent oscillations synchronized with the load fluctuations. In contrast, the switching-reference control substantially reduces both the magnitude and persistence of control actions after a short transient. The voltage remains consistently within the admissible 5% voltage-deviation band and closer to the nominal value.

Next, we conduct simulations with two data centers at buses 22 and 25, respectively, each running AI training workloads. Fig. 4 shows that the proposed switching-reference controller continues to suppress switching-induced voltage deviations caused by power fluctuations from the two data centers. In contrast, conventional fixed-reference control incurs large reactive power control effort and frequent voltage

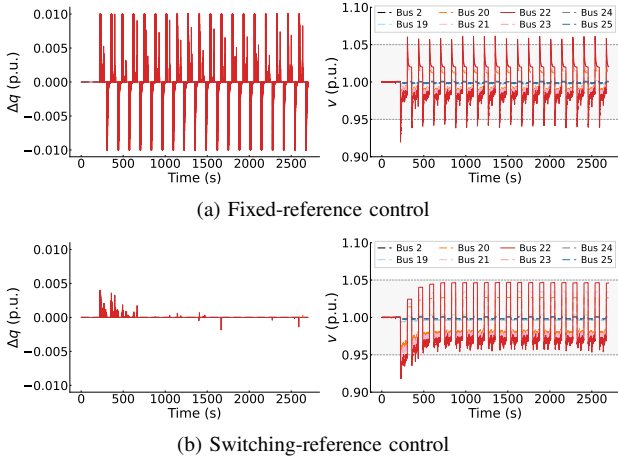


Fig. 3. Single data center scenario: comparison of incremental reactive adjustment  $\Delta q$  (p.u.) and voltage trajectory  $v$  (p.u.) under droop control with a fixed reference and a switching reference. The proposed switching-reference control substantially reduces control effort in reactive power while maintaining voltage in admissible 5% voltage-deviation band.

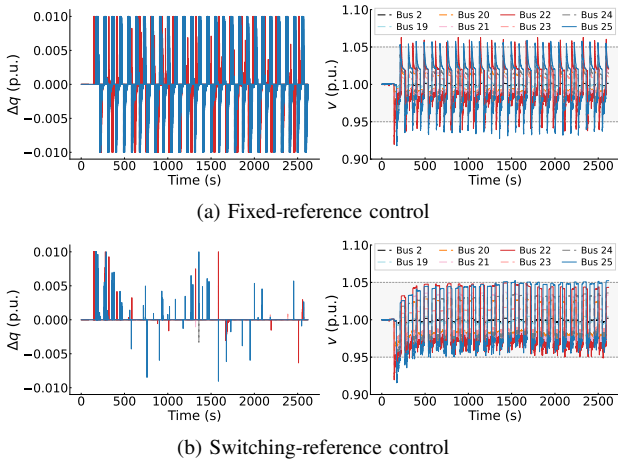


Fig. 4. Two data center scenario: comparison of incremental reactive adjustment  $\Delta q$  (p.u.) and voltage trajectory  $v$  (p.u.) under droop control with a fixed reference and a switching reference. The proposed switching-reference control remains effective even when multiple data center loads introduce simultaneous switching disturbances.

violations. These results indicate that the proposed method remains effective even when multiple data center loads introduce simultaneous switching disturbances within the feeder. Overall, the switching reference substantially reduces both reactive power control effort and voltage deviations across switching cycles.

### C. Compatibility with Data Center Load Smoothing

To examine compatibility with potential load-smoothing control in the data center, we simulate a case in which the data center initially operates without internal power regulation and starts internal load smoothing at  $t \approx 1400$ s. The power trace therefore allow us to assess whether the proposed controller can promptly adapt to changes in the power profile induced by internal load-smoothing control.

Specifically, the data center is modeled as a single aggregated load equipped with an energy storage system, where the storage is sized to supply the maximum data center power for 60s, corresponding to the time required

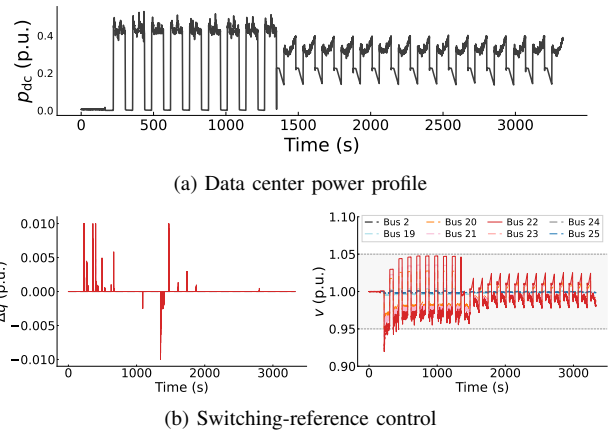


Fig. 5. Decentralized grid-side voltage control with internal data center load smoothing. (a) Data center power profile with internal load smoothing starting at  $t \approx 1400$ s. (b) Reactive control actions  $\Delta q$  (p.u.) and voltage trajectories  $v$  (p.u.) under the proposed switching-reference controller.

for backup generators to come online. The storage dispatch changes the net active power injection at the data center bus as  $\hat{p}_{j,t} = p_{j,t} - z_{j,t}$ , where  $z_{j,t}$  denotes the storage dispatch power. Its dispatch follows a simple droop-type rule that compensates for deviations from the recent average load:  $z_{j,t} = -k_p \left( p_{j,t} - \frac{1}{T} \sum_{\tau=t-T}^t p_{j,\tau} \right)$  with droop gain  $k_p = 0.6$  and averaging horizon  $T = 100$ s. To preserve backup capability, the storage is restricted to operate within a narrow state-of-charge band around 95% (0.93–0.97), and the dispatch is forced to zero whenever these energy limits are reached.

The data center power profile is shown in Fig. 5(a), where the power trace during the initial period follows the original switching pattern of the training workload and exhibits a reduced magnitude of power transitions after smoothing begins. The corresponding voltage trajectory and control actions are shown in Fig. 5(b). After load smoothing is activated in the data center, the reduced power fluctuations lead to smaller voltage deviations, and the controller exhibits only mild control actions. These results illustrate that the proposed controller remains effective without requiring extensive coordination when the load switching pattern is altered by load smoothing in the data center.

## V. CONCLUSIONS

This paper studies voltage regulation in distribution systems subject to rapid and periodic power fluctuations induced by large-scale AI training workloads. A decentralized switching-reference voltage control framework is developed to exploit the two-mode structure of AI training workloads. Conditions for voltage convergence are established, and the measurement-based switching-reference design is characterized to reduce worst-case voltage deviations.

Simulation studies on the IEEE 33-bus feeder demonstrate that the proposed method substantially reduces both voltage deviations and reactive power control effort compared with conventional droop control. The controller remains effective in scenarios involving multiple data centers and when coordinated with load smoothing in data centers.

## REFERENCES

- [1] J. Kaplan, S. McCandlish, T. Henighan, T. B. Brown, B. Chess, R. Child, S. Gray, A. Radford, J. Wu, and D. Amodei, "Scaling laws for neural language models," *arXiv preprint arXiv:2001.08361*, 2020.
- [2] J. Hoffmann, S. Borgeaud, A. Mensch, E. Buchatskaya, T. Cai, E. Rutherford, D. Casas, L. A. Hendricks, J. Welbl, A. Clark *et al.*, "Training compute-optimal large language models," *arXiv preprint arXiv:2203.15556*, vol. 10, 2022.
- [3] I. E. Agency, "Energy and ai," <https://www.iea.org/reports/energy-and-ai>, 2025.
- [4] E. Choukse, B. Warriar, S. Heath, L. Belmont, A. Zhao, H. A. Khan, B. Harry, M. Kappel, R. J. Hewett, K. Datta *et al.*, "Power stabilization for ai training datacenters," *arXiv preprint arXiv:2508.14318*, 2025.
- [5] Photovoltaics, Distributed Generation and Storage, Energy, "Standard for interconnection and interoperability of distributed energy resources with associated electric power systems interfaces," *IEEE Standards*, 2018.
- [6] H. Zhu and H. J. Liu, "Fast local voltage control under limited reactive power: Optimality and stability analysis," *IEEE Transactions on Power Systems*, vol. 31, no. 5, pp. 3794–3803, 2015.
- [7] K. Baker, A. Bernstein, E. Dall'Anese, and C. Zhao, "Network-cognizant voltage droop control for distribution grids," *IEEE Transactions on Power Systems*, vol. 33, no. 2, pp. 2098–2108, 2018.
- [8] W. Cui, Y. Xie, S. Low, A. Wierman, and B. Zhang, "Leveraging predictions in power system voltage control: An adaptive approach," *arXiv preprint arXiv:2509.09937*, 2025.
- [9] V. Sakalkar, V. Kontorinis, D. Landhuis, S. Li, D. De Ronde, T. Blooming, A. Ramesh, J. Kennedy, C. Malone, J. Clidaras *et al.*, "Data center power oversubscription with a medium voltage power plane and priority-aware capping," in *Proceedings of the Twenty-Fifth International Conference on Architectural Support for Programming Languages and Operating Systems*, 2020, pp. 497–511.
- [10] S. Hou, W. Ni, S. Zhao, B. Cheng, S. Chen, and J. Chen, "Decentralized real-time optimization of voltage reconfigurable cloud computing data center," *IEEE Transactions on Green Communications and Networking*, vol. 4, no. 2, pp. 577–592, 2020.
- [11] Y. Chen and B. Zhang, "Voltage regulation in distribution systems with data center loads," *arXiv preprint arXiv:2507.06416*, 2025.
- [12] Y. Xie, W. Cui, and A. Wierman, "Enhancing data center low-voltage ride-through," *arXiv preprint arXiv:2510.03867*, 2025.
- [13] Z. Liang, J.-W. Chung, M. Chowdhury, J. Chen, and V. Dvorkin, "Gpu-to-grid: Voltage regulation via gpu utilization control," *arXiv preprint arXiv:2602.05116*, 2026.
- [14] A. Azizi, S. Morovati, A. Zamani, J. Piruzza, D. Guo, Z. Liu, and P. Taimela, "Strengthening data center operations using grid-forming battery energy storage as a line-interactive uninterruptible power supply," *International Journal of Electrical Power & Energy Systems*, vol. 175, p. 111638, 2026.
- [15] B. A. Ross, X. Lyu, U. C. Nwaneto, S. M. Mohiuddin, and A. B. Nasrif, "Using grid-forming energy storage systems to provide dynamic active power support for hyperscale data center," *IEEE Access*, 2026.
- [16] Y. Fan, X. Tao, Z. Ye, K. Kumar, and R. Gadh, "From co-location to coordination: Ev aggregator dispatch for voltage regulation of ai data center-integrated distribution systems," *Available at SSRN 6346298*, 2026.
- [17] M. Baran and F. Wu, "Network reconfiguration in distribution systems for loss reduction and load balancing," *IEEE Transactions on Power Delivery*, vol. 4, no. 2, pp. 1401–1407, 1989.
- [18] ANSI/NEMA, *American National Standard for Electric Power Systems and Equipment-Voltage Ratings (60 Hertz)*. National Electrical Manufacturers Association, 2025.
- [19] W. Cui, J. Li, and B. Zhang, "Decentralized safe reinforcement learning for inverter-based voltage control," *Electric Power Systems Research*, vol. 211, p. 108609, 2022.
- [20] Y. Shi, B. Xu, D. Wang, and B. Zhang, "Using battery storage for peak shaving and frequency regulation: Joint optimization for superlinear gains," *IEEE transactions on power systems*, vol. 33, no. 3, pp. 2882–2894, 2017.
- [21] X. Yuan, J. Hu, and S. Cheng, "Multi-time scale dynamics in power electronics-dominated power systems," *Frontiers of Mechanical Engineering*, vol. 12, no. 3, pp. 303–311, 2017.
- [22] H. Touvron, L. Martin, K. Stone, P. Albert, A. Almahairi, Y. Babaei, N. Bashlykov, S. Batra, P. Bhargava, S. Bhosale *et al.*, "Llama 2: Open foundation and fine-tuned chat models," *arXiv preprint arXiv:2307.09288*, 2023.
- [23] T. Dettmers, A. Pagnoni, A. Holtzman, and L. Zettlemoyer, "Qlora: Efficient finetuning of quantized llms," *Advances in neural information processing systems*, vol. 36, pp. 10 088–10 115, 2023.

## APPENDIX

### A. Derivation of the Error Dynamics

Starting from the definition

$$\mathbf{e}_t := \mathbf{v}_t - \mathbf{v}_t^{\text{ref}},$$

we derive the deviation recursion (8). Recall the voltage model (1) and the droop update (4):

$$\mathbf{v}_t = \mathbf{R}\mathbf{p}_t + \mathbf{X}\mathbf{q}_t, \quad \mathbf{q}_{t+1} = \mathbf{q}_t - \mathbf{K}(\mathbf{v}_t - \mathbf{v}_t^{\text{ref}}) = \mathbf{q}_t - \mathbf{K}\mathbf{e}_t.$$

Then

$$\begin{aligned} \mathbf{e}_{t+1} &= \mathbf{v}_{t+1} - \mathbf{v}_{t+1}^{\text{ref}} \\ &= \mathbf{R}\mathbf{p}_{t+1} + \mathbf{X}\mathbf{q}_{t+1} - \mathbf{v}_{t+1}^{\text{ref}} \\ &= \mathbf{R}\mathbf{p}_{t+1} + \mathbf{X}(\mathbf{q}_t - \mathbf{K}\mathbf{e}_t) - \mathbf{v}_{t+1}^{\text{ref}} \\ &= \mathbf{R}\mathbf{p}_{t+1} + \mathbf{X}\mathbf{q}_t - \mathbf{X}\mathbf{K}\mathbf{e}_t - \mathbf{v}_{t+1}^{\text{ref}} \\ &= \mathbf{R}\mathbf{p}_{t+1} + (\mathbf{v}_t - \mathbf{R}\mathbf{p}_t) - \mathbf{X}\mathbf{K}\mathbf{e}_t - \mathbf{v}_{t+1}^{\text{ref}} \\ &= \mathbf{R}\mathbf{p}_{t+1} + (\mathbf{e}_t + \mathbf{v}_t^{\text{ref}} - \mathbf{R}\mathbf{p}_t) - \mathbf{X}\mathbf{K}\mathbf{e}_t - \mathbf{v}_{t+1}^{\text{ref}} \\ &= (\mathbf{I} - \mathbf{X}\mathbf{K})\mathbf{e}_t + \mathbf{R}(\mathbf{p}_{t+1} - \mathbf{p}_t) - (\mathbf{v}_{t+1}^{\text{ref}} - \mathbf{v}_t^{\text{ref}}) \\ &= (\mathbf{I} - \mathbf{X}\mathbf{K})\mathbf{e}_t + \mathbf{R}\Delta\mathbf{p}_t - \Delta\mathbf{v}_t^{\text{ref}}. \end{aligned}$$

### B. Gain condition for contraction of $\mathbf{I} - \mathbf{X}\mathbf{K}$

**Lemma 4.** Assume  $\mathbf{X} = \mathbf{X}^\top \succ 0$  and the diagonal matrix  $\mathbf{K}$  satisfies  $0 \prec \mathbf{K} \prec 2\mathbf{X}^{-1}$ . Let  $\mathbf{A} := \mathbf{I} - \mathbf{X}\mathbf{K}$ . Then there exist a nonnegative matrix  $\mathbf{C}$  and a constant  $0 < \epsilon < 1$  such that

$$|\mathbf{A}^k| \leq \mathbf{C}\epsilon^k, \quad \forall k \geq 0.$$

*Proof.* From  $0 \prec \mathbf{K} \prec 2\mathbf{X}^{-1}$  and  $\mathbf{X} \succ 0$ , it follows that  $0 \prec \mathbf{X}^{1/2}\mathbf{K}\mathbf{X}^{1/2} \prec 2\mathbf{I}$  [19]. Hence all eigenvalues of  $\mathbf{I} - \mathbf{X}^{1/2}\mathbf{K}\mathbf{X}^{1/2}$  lie in  $(-1, 1)$ .

Moreover,

$$\mathbf{A} = \mathbf{X}^{-1/2}(\mathbf{I} - \mathbf{X}^{1/2}\mathbf{K}\mathbf{X}^{1/2})\mathbf{X}^{1/2},$$

so  $\mathbf{A}$  is similar to the symmetric matrix  $\mathbf{I} - \mathbf{X}^{1/2}\mathbf{K}\mathbf{X}^{1/2}$ . Let  $\epsilon := \rho(\mathbf{A}) < 1$ . Then there exists an invertible matrix  $\mathbf{P}$  such that  $\mathbf{A} = \mathbf{P}\Lambda\mathbf{P}^{-1}$  with  $|\lambda_i| \leq \epsilon$ .

Using  $|\mathbf{A}\mathbf{B}| \leq |\mathbf{A}||\mathbf{B}|$  and  $|\Lambda|^k \leq \epsilon^k\mathbf{I}$  gives

$$|\mathbf{A}^k| = |\mathbf{P}\Lambda^k\mathbf{P}^{-1}| \leq |\mathbf{P}||\Lambda|^k|\mathbf{P}^{-1}| \leq |\mathbf{P}||\mathbf{P}^{-1}|\epsilon^k.$$

The claim follows by taking  $\mathbf{C} := |\mathbf{P}||\mathbf{P}^{-1}|$ .  $\square$